


## SPECIAL ISSUE RESEARCH ARTICLE

# Multi-contrast volumetric imaging with isotropic resolution for assessing infarct heterogeneity: Initial clinical experience

Li Zhang<sup>1,2</sup>  | Peng Lai<sup>3</sup> | Idan Roifman<sup>4</sup> | Mihaela Pop<sup>1,2,4</sup> | Graham A. Wright<sup>1,2,4</sup><sup>1</sup>Department of Medical Biophysics, University of Toronto, Toronto, Ontario, Canada<sup>2</sup>Physical Sciences Platform, Sunnybrook Research Institute, Toronto, Ontario, Canada<sup>3</sup>Global Applied Science Laboratory, GE Healthcare, Menlo Park, California, USA<sup>4</sup>Schulich Heart Research Program, Sunnybrook Research Institute, Toronto, Ontario, Canada**Correspondence**Graham Wright, Sunnybrook Health Sciences Centre, 2075 Bayview Avenue, Room M7-611, Toronto, Ontario M4N 3M5, Canada.  
Email: graham.wright@sri.utoronto.ca**Funding information**

Canadian Institutes of Health Research, Grant/Award Number: MOP-93531; GE Healthcare; Ontario Research Fund

**Background.** To evaluate accelerated multi-contrast volumetric imaging with isotropic resolution reconstructed using low-rank and spatially varying edge-preserving constrained compressed sensing parallel imaging reconstruction (CP-LASER), for assessing infarct heterogeneity on post-infarction patients as a precursor to studies of utility for predicting ventricular arrhythmias.**Methods.** Eleven patients with prior myocardial infarction were included in the study. All subjects underwent cardiovascular magnetic resonance (CMR) scans including conventional two-dimensional late gadolinium enhancement (2D LGE) and three-dimensional multi-contrast late enhancement (3D MCLE) post-contrast. The extent of the infarct core and peri-infarct gray zone of a limited mid-ventricular slab were derived respectively by analyzing MCLE images with an isotropic resolution of 2.2 mm and an anisotropic resolution of  $2.2 \times 2.2 \times 8.8$  mm<sup>3</sup>, and LGE images with a resolution of  $1.37 \times 2.7 \times 8$  mm<sup>3</sup>; the respective measures across all subjects were statistically compared.**Results.** Using 3D MCLE, the infarct core size measured with isotropic resolution was similar to that measured with anisotropic resolution, while the peri-infarct gray zone size measured with isotropic resolution was smaller than that measured with anisotropic resolution ( $p < 0.001$ , Cohen's  $d_z = 1.33$ ). Isotropic 3D MCLE yielded a significantly smaller measure of the peri-infarct gray zone size than conventional 2D LGE ( $p = 0.0016$ , Cohen's  $d_z = 1.20$ ). Overall, we have successfully shown the utility of isotropic 3D MCLE in a pilot patient study. Our results suggest that smaller voxels lead to more accurate differentiation between isotropic 3D MCLE-derived gray zone and core infarct because of diminished partial volume effect.**Conclusion.** The CP-LASER accelerated 3D MCLE with isotropic resolution can be used in patients and yields excellent delineation of infarct and peri-infarct gray zone characteristics.**KEYWORDS**

compressed sensing, infarct heterogeneity, isotropic resolution, late gadolinium enhancement, multi-contrast imaging, partial volume effects

## 1 | BACKGROUND

Sudden cardiac death (SCD) is a leading cause of cardiac mortality in the United States<sup>1</sup> and is primarily attributed to malignant ventricular arrhythmias associated with prior myocardial infarction (MI), including ventricular tachycardia (VT) or fibrillation (VF).<sup>2</sup> Implantable cardioverter

**Abbreviations:** CMR, cardiovascular magnetic resonance; CNR, contrast-to-noise ratio; CP-LASER, compressed sensing parallel imaging reconstruction; DICOM, Digital Imaging and Communications in Medicine; DTPA, Diethylenetriaminepentaacetic acid; ECG, electrocardiogram; FGRE, fast gradient echo; FOV, Field of view; FGRE, fast gradient echo; FWHM, full-width half maximum; ICD, implantable cardioverter defibrillator; IR, inversion recovery; LGE, late gadolinium enhancement; LOST, low-dimensional-structure self-learning and thresholding; LV, left ventricle; LVEDV, left ventricular end diastolic volume; LVEF, left ventricular ejection fraction; LVESV, left ventricular end systolic volume; MCLE, multi-contrast late enhancement; MI, myocardial infarction;  $M_{ss}$ , steady-state magnetization; RF, radiofrequency; SCD, sudden cardiac death; SI, signal intensity; SSFP, steady-state free precession;  $T_1^*$ , apparent  $T_1$  relaxation; TE, Echo time; TI, inversion time; TR, Repetition time; VF, ventricular fibrillation; VPS, views per segment; VT, ventricular tachycardia

defibrillators (ICDs) can effectively terminate most episodes of VT/VF and are considered for primary prevention of sudden death in post-infarction patients with a low left ventricular ejection fraction (LVEF). Currently, the clinical standard approach to identifying appropriate candidacy for ICD implantation relies on impaired LVEF  $\leq 35\%$  as the primary index.<sup>3,4</sup> However, only a 5% annual incidence of appropriate ICD firings has been reported on the patients selected by this approach for primary prevention of SCD<sup>5</sup> and it fails in identifying the patients who undergo the majority of SCD events.<sup>6</sup> Direct assessment of the underlying arrhythmic substrate using CMR has shown the potential to facilitate risk stratification of patients with prior MI for appropriate ICD implantation.<sup>7-12</sup> The critical isthmuses of VTs have been located in the peri-infarct zone identified using CMR (i.e. gray zone) in patients with prior MI.<sup>13,14</sup> Furthermore, the extent of infarct heterogeneity assessed by CMR predicts the occurrence of VT/VF post-MI, motivating ICD implantation.<sup>8,9,11</sup> However, the measure of peri-infarct gray zone varies in size with degradation of imaging resolution due to partial volume effects, which has been substantiated in preclinical studies with comparison to histopathology.<sup>15,16</sup> Recent clinical studies of VT patients with prior MI have demonstrated that the gray zone channels identified using three-dimensional late gadolinium enhancement (3D LGE) with an isotropic resolution on the level of 1.5 mm matched the majority of the critical VT isthmuses identified with electrophysiology mapping techniques, while two-dimensional (2D) LGE with a slice thickness of 5 mm yielded a lower matching rate.<sup>17,18</sup> Therefore, volumetric imaging with a high spatial resolution is preferable for accurate assessment of infarct heterogeneity for patient risk stratification to indicate appropriate ICD therapy.

2D LGE has become the clinical gold standard for MI visualization<sup>19,20</sup> and can identify infarct heterogeneity by quantifying relative differences in signal intensities within the infarct territory using a variety of thresholding methods.<sup>7,21,22</sup> Multi-contrast late enhancement (MCLE) is an alternative technique that provides multi-contrast visualization of MI<sup>23</sup> and uses a data clustering method to identify infarct heterogeneity.<sup>24</sup> In several clinical studies, 2D MCLE has demonstrated clinical benefits over conventional 2D LGE in terms of the sensitivity of MI detection and the robustness of infarct heterogeneity characterization.<sup>25-27</sup> To maximize the clinical utility of MCLE in infarct heterogeneity assessment, a 3D version is implemented to provide continuous coverage of MI, avoiding slice misregistration due to inconsistent breath-hold positions over multiple single-slice MCLE scans, and to achieve increased spatial resolution to minimize the partial volume effect on gray zone measurement. Under the restrictions posed by limited acquisition time and contrast agent kinetics, a highly accelerated acquisition is needed for 3D MCLE to acquire isotropic resolution in a single breath-hold or a short free-breathing scan.<sup>28</sup> Recently, a low-rank and spatially varying edge-preserving constrained compressed sensing parallel imaging reconstruction method (CP-LASER) was developed to effectively preserve contrast of small features from accelerated multi-contrast volumetric imaging for cases of varying contrast-to-noise ratio (CNR), ensuring accurate reconstruction of fine image features in the peri-infarct zone using isotropic 3D MCLE.<sup>29</sup> This method has demonstrated robust multi-contrast reconstruction of peri-infarct characteristics with excellent correspondence with histopathology in a preclinical study using 3D MCLE with an isotropic resolution of 1.5 mm, acquired in a single breath-hold scan. In a clinical demonstration on a patient with prior MI, 3D MCLE with an isotropic resolution using CP-LASER has shown obvious variations of peri-infarct characteristics across adjacent 2.2-mm-thick short-axis slices, which conventional 2D LGE was not able to recognize due to the partial volume effect occurring with a slice thickness of 8 mm. In this work, we hypothesize that isotropic 3D MCLE can provide improved assessment of infarct heterogeneity on patients with prior MI, compared with conventional 2D LGE and 3D MCLE with anisotropic resolution that is inferior in the through-plane dimension. The objective of this study is to translate isotropic 3D MCLE toward clinical utility in infarct heterogeneity assessment.

## 2 | METHODS

### 2.1 | Patient Population

Eleven post-infarction patients with coronary artery disease were enrolled for a detailed CMR assessment from April 2015 to September 2017 in studies approved by our institutional research ethics board. Informed consent was obtained in all subjects.

### 2.2 | Imaging Protocol

All CMR scans were performed on a GE 1.5T scanner with electrocardiogram (ECG) gating and using a 30-channel cardiac coil array (GE Healthcare, Waukesha, MI). The imaging protocol included cardiac cine pre-contrast, as well as cine inversion recovery (cine IR), conventional 2D LGE and accelerated 3D MCLE post-contrast. Cardiac cine acquired short-axis slices covering the entire left ventricle (LV) prescribed based on a 3-plane localizer. Post-contrast imaging was performed starting from 8 minutes after injection of 0.2mmol/kg Gadolinium-DTPA (Magnevist; Berlex Inc., Wayne, NJ, USA). LGE images were acquired right after cine IR imaging and MCLE was performed 10-20 minutes after LGE. Using the same short-axis localization as cardiac cine imaging, LGE and MCLE were prescribed to cover the infarct region.

Cardiac cine uses steady-state free precession (SSFP) with the following parameters: TR/TE = 4.6/1.9 ms, flip angle = 60°, receiver bandwidth = 83.3 kHz, field of view (FOV) = 35 cm, acquisition matrix = 256 × 256, slice thickness = 8 mm, views per segment (VPS) = 16, number of phases = 20. LV functional parameters including LVEF, left ventricular end diastolic volume (LVEDV) and end systolic volume (LVESV) were measured on cardiac cine images using CMR<sup>42</sup> software (Circle Cardiovascular Imaging, Calgary, Canada).

Cine IR uses multiphase fast gradient echo (FGRE) cine acquisition after an inversion recovery (IR) pulse, and captures image contrast change at different inversion times (TIs), facilitating determination of the optimal TI value for LGE. The parameters for cine IR included: TR/TE = 4.5/2.0

ms, flip angle = 5°, receiver bandwidth = 31.25 kHz, FOV = 35 cm, acquisition matrix = 128 × 128, slice thickness = 8 mm, VPS = 8, number of phases = 50, number of R-R intervals = 1.

Conventional 2D LGE uses an IR-FGRE sequence. With cine IR images as reference, the optimal TI value in LGE was determined for each subject by selecting the null point for healthy myocardium, and it varied from 200 to 300 ms. LGE parameters were as follows: TR/TE = 5.9/1.6 ms, flip angle = 15°, receiver bandwidth = 22.5 kHz, FOV = 35 cm, acquisition matrix = 256 × 128, slice thickness = 8 mm. Due to a given Digital Imaging and Communications in Medicine (DICOM) format, LGE images were interpolated into a 256 × 256 matrix before analysis.

The 3D MCLE sequence uses a segmented SSFP readout following an IR pulse. Variable density Poisson-disc sampling was implemented to sparsely sample the 3D k-space with a net acceleration rate of 5, facilitating acquisition of a 3D slab in a single breath-hold. Sampling patterns varied for acquisitions at different inversion times. The accelerated 3D MCLE used the following parameters: TR = 3.2 or 3.4 ms, TE = 1.4 ms, flip angle = 45°, receiver bandwidth = 125 kHz, FOV = 35 cm, acquisition matrix = 160 × 160 × 10, slice thickness = 2.2 mm, number of slices in a single 3D slab = 10, VPS = 16, number of TIs = 5 or 6. Multi-contrast images were acquired at the inversion times in the range between 60 ms and 340 ms.

For both conventional 2D LGE and 3D MCLE, the trigger delay was adjusted for each subject, using pre-contrast cine images as reference so that the acquisition happened during the diastolic periods to minimize cardiac motion. Images were acquired during breath-holds of 15-20 seconds. For 2D imaging including cardiac cine as well as cine IR and LGE, each slice was acquired in a single breath-hold. 3D MCLE acquired each slab covering 10 slices in a single breath-hold.

### 2.3 | Image Reconstruction for 3D MCLE

The CP-LASER method was developed to effectively preserve contrast of small-scale structures in CNR-limited scenarios, particularly for infarct heterogeneity characterization, when reconstructing multi-contrast image volumes from undersampled data (here, a five-fold accelerated 3D MCLE acquisition). Such contrast loss is a challenge to any sparse-model based reconstruction in cases of low CNR and high accelerations.

The detailed explanation for CP-LASER and the approach for selecting its regularization parameter  $\lambda$  have been previously described.<sup>28,29</sup> Briefly, CP-LASER synergistically integrates low-rank temporal MR relaxation signal behavior (via principal component analysis on a training matrix or on fully sampled low-order k-space at different inversion times) and low-rank spatial sensitivity profiles of receiver coils (via the ESPIRiT eigenvalue-based method<sup>30</sup>) for signal denoising. This is followed by iterative compressed sensing reconstruction at progressively finer spatial scales, enforcing spatial sparsity in images via a weighted total variation regularization function. Spatially varying weights within this function are calculated from the spatial gradients in the image volume at each iteration to minimize regularization in the vicinity of 'edges'. The relative emphasis on regularization versus data fidelity is further tuned at a global scale via  $\lambda$ .

Generally, one expects greater image smoothing with greater emphasis on regularization, although this is mitigated to some extent by edge-preserving constraints. Since image smoothing could increase apparent gray zone, we evaluated the effect of changes in  $\lambda$  on the gray zone size calculation.

For a succinct description, an appropriate  $\lambda$  was selected to facilitate suppressing artifacts and noise while not over-regularizing the reconstruction. In this work, the selected regularization parameter  $\lambda_0$  was  $8 \times 10^{-4}$ .

Using 3D MCLE, a 2.2-cm-thick short-axis slab comprising 10 slices in the infarct territory were reconstructed for each of 10 subjects and two slabs covering different infarct regions were reconstructed for the 11th subject. Given the slab boundary artifacts due to imperfect slab-selective radiofrequency (RF) pulse profiles, 2 slices at each edge of the slab were excluded from the analysis following the image reconstruction, leaving the central 6 slices for analysis. Our approach to producing MCLE images with an anisotropic resolution of  $2.2 \times 2.2 \times 8.8 \text{ mm}^3$  was to average 4 consecutive 3D MCLE slices. By this means, multi-contrast images for 3 slices with such anisotropic resolution were produced for each slab, which corresponded respectively with the first, central and last 4 slices in the six slices. All the reconstructed MCLE images were interpolated into a 256 × 256 matrix for the following analysis.

### 2.4 | Infarct Heterogeneity Analysis

Infarct heterogeneity analysis in LGE uses a full-width half-maximum method (FWHM) to distinguish peri-infarct gray zone from infarct core in an infarct region.<sup>7,24</sup> Epicardial and endocardial contours were drawn manually to segment out pixels from the left ventricle. Papillary muscle infarcts located in the LV blood pool were manually drawn as separate infarct regions and were included in the analysis. A region of remote myocardium was chosen as a reference region free of artifacts and with uniform myocardial suppression, and the peak signal intensity of this region ( $\text{Peak}_{\text{remote}}$ ) was calculated. Similarly, the maximum intensity region of the myocardium was chosen as the infarct and the peak signal intensity among all pixels in the infarct regions ( $\text{Peak}_{\text{infarct}}$ ) was determined. The signal intensity (SI) thresholds for determining the infarct core and peri-infarct gray zone using FWHM were as follows:  $\text{SI}_{\text{core}} > 0.5 * \text{Peak}_{\text{infarct}}$  and  $\text{Peak}_{\text{remote}} < \text{SI}_{\text{grayzone}} < 0.5 * \text{Peak}_{\text{infarct}}$ , where  $\text{SI}_{\text{core}}$  is the signal intensity of a pixel classified as the infarct core and  $\text{SI}_{\text{grayzone}}$  is the signal intensity of a pixel classified as the peri-infarct gray zone.<sup>7,31</sup>

In the multi-contrast volumetric images, signal characteristics over multiple TIs for a single voxel can be represented by two tissue-dependent MR parameters including the apparent  $T_1$  relaxation ( $T_1^*$ ) and steady-state magnetization ( $M_{\text{ss}}$ ).<sup>28</sup> In this study, the two MR parameters were calculated by fitting voxel-wise signal intensities at six inversion times into a parametric exponential recovery model. The fuzzy C-means clustering method was then applied to a scatter plot of  $T_1^*$  and  $M_{\text{ss}}$  for voxels of interest to calculate the probability of each voxel belonging to infarct, healthy

myocardium or blood. The infarct core and healthy myocardium were determined as the voxels with a probability greater than 75% of belonging to infarct or healthy myocardium, respectively. The peri-infarct gray zone was determined as the voxels with less than a 75% probability of belonging to one of the two clusters (including infarct and healthy myocardium) and greater than a 25% probability for belonging to the other one.<sup>24,27</sup>

## 2.5 | Evaluation & Comparison

Following infarct heterogeneity analysis, all the measures of the infarct core and peri-infarct gray zone were expressed in grams of tissue. This is the clinically accepted standard measure; to convert to cubic centimetres, we may scale by the tissue density ( $\sim 1 \text{ g/cm}^3$ ), and then divide by the slice thickness to obtain areas.

In previous preclinical MR and histopathological studies, we demonstrated that edema and inflammation resorb almost completely after 5–6 weeks post-MI.<sup>32,33</sup> As all the infarcts in this study were more than one month old, the conversion above was sufficient.

### 2.5.1 | Effect of $\lambda$ on Gray Zone Measure

The peri-infarct gray zone size for each of the central 4 slices with isotropic resolution in each MCLE slab reconstructed with different regularization parameters was calculated and compared to assess sensitivity to parameter selection. The regularization parameters under evaluation included the selected  $\lambda_0$  and the values that are smaller and larger than  $\lambda_0$  by 25%.

### 2.5.2 | Isotropic versus Anisotropic 3D MCLE

The total sizes of the infarct core and peri-infarct gray zone of the central 4 slices with an isotropic resolution of 2.2 mm for each MCLE slab were calculated and compared with those of the corresponding slice with an anisotropic resolution of  $2.2 \times 2.2 \times 8.8 \text{ mm}^3$  to assess impact of partial volume effects.

### 2.5.3 | Isotropic 3D MCLE versus Conventional 2D LGE

For each MCLE slab, the 8-mm-thick LGE slices with locations in the range of the six MCLE slices with isotropic 2.2-mm resolution were selected and aligned to these isotropic MCLE slices using the slice location information. A stack of four consecutive isotropic MCLE slices was paired with a given LGE slice by choosing the stack with a minimal location difference from the LGE slice among the six MCLE slices. The central location of a stack was used for calculating the location difference from a given LGE slice. For each MCLE slab, only the pair of a LGE slice and a stack of 4 consecutive MCLE slices with the smallest distance in location was chosen for analysis and considered geometrically corresponding (overall average location difference  $0.28 \pm 0.40 \text{ mm}$ ). The total sizes of the infarct core and peri-infarct gray zone of the 4 consecutive MCLE slices in a chosen pair were calculated and compared to those of the corresponding LGE slice.

## 2.6 | Statistical Analysis

Data were analyzed for all subjects with LGE and MCLE. The measures of the infarct core and peri-infarct gray zone across all subjects using different methods were compared using regression and correlation analysis, the Bland-Altman analysis and the paired Student's t-test. A p-value less than 0.05, calculated from the paired Student's t-test, was considered as having a statistical significance. For the regression and correlation analysis, the slope, intercept, correlation coefficient (Pearson's  $r$ ) and root-mean-square error (RMSE) were calculated for each comparison. Effect sizes were calculated with Cohen's  $d_z$  for paired samples and reported where they were large ( $\geq 0.8$ ).

Image reconstruction and all following analyses were performed in MATLAB (MathWorks, Natick, MA, USA). The statistics toolbox in MATLAB was used for statistical analysis.

## 3 | RESULTS

Baseline characteristics of our cohort are summarized in Table 1. In the cohort, the average age was  $60 \pm 14$  (means  $\pm$  SD) and 45.5% of our patients were male. All the patients had previous MI more than 1 month old and mean LVEF at baseline was  $42 \pm 11\%$ . The average heart rate during imaging was  $56 \pm 5 \text{ bpm}$  (range: 49–65 bpm).

Figure 1 shows CMR images for a short-axis slice on a 44-year-old male acquired 27 weeks after MI. MCLE images at different inversion times yielded varying tissue contrast and the dark blood image at the inversion time of 214.4 ms provided better visualization of the sub-endocardial infarct than the LGE image, where the infarct presented similar signal to that of adjacent blood.

Figure 2 shows CMR images and the resulting segmentation of the infarct core and peri-infarct gray zone for a mid-ventricular short-axis slice on a 62-year-old female acquired 26 weeks after MI. This example demonstrated the inferior wall myocardial infarction with involvement of both papillary muscles, clearly seen from the dark blood MCLE image in Figure 2C. Our LGE analysis produced more gray zone pixels than isotropic MCLE, especially in the peri-infarct zone along the inferior epicardial border.

Figure 3 demonstrates the segmentation results of the infarct core and peri-infarct gray zone using different methods for a given infarct region on the same patient as in Figure 1. With high isotropic resolution, MCLE was able to identify the variations of the peri-infarct characteristics across multiple 2.2-mm-thick consecutive slices, which were not recognized using conventional 2D LGE and MCLE with anisotropic resolution

that was inferior in the through-plane dimension. Both conventional 2D LGE or MCLE with anisotropic resolution yielded more peri-infarct gray zone pixels than the individual MCLE slice with isotropic resolution that was visually closest to them, likely due to the partial volume effect occurring with a thicker slice thickness on the order of 8 mm.

Figure 4 compares the measures of the peri-infarct gray zone size of a single 2.2-mm-thick MCLE slice using different regularization parameters across 4 slices for each of 11 subjects. There is excellent agreement between the gray zone size measure using  $\lambda_0$  and that using a regularization parameter either larger ( $r = 0.94, p = 0.81$ ) or smaller ( $r = 0.95, p = 0.31$ ) than  $\lambda_0$  by 25% with no statistically significant differences in either comparison. As seen in Figure 4, there is no clear effect of increasing or decreasing  $\lambda$  on gray zone size, demonstrating that choice of the precise value of this parameter is not critical to this measurement.

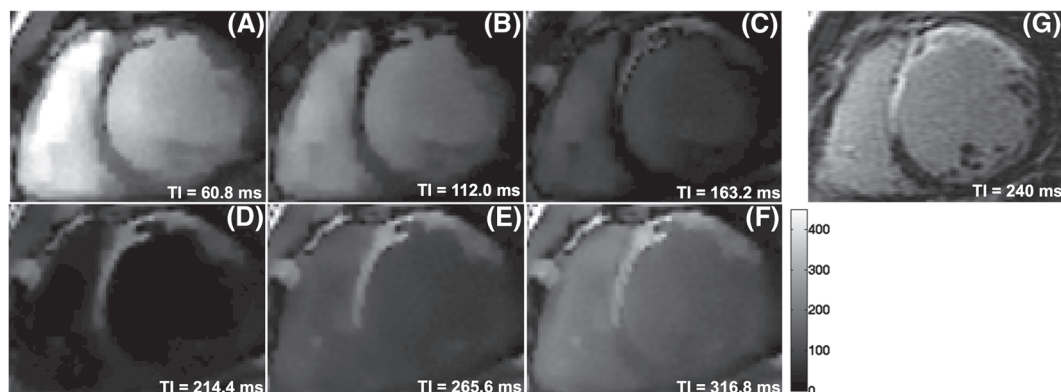
Figure 5 compares MCLE measures in the infarct core and peri-infarct gray zone size of a 8.8-mm-thick short-axis slice between using an isotropic resolution of 2.2 mm and using an anisotropic resolution of  $2.2 \times 2.2 \times 8.8 \text{ mm}^3$ . For MCLE measures of the infarct core size, there was good agreement between using anisotropic resolution and isotropic resolution ( $r = 0.86, p = 0.43$ ) and no bias detected using the Bland-Altman analysis. The peri-infarct gray zone size measured using anisotropic resolution was significantly larger than that measured using isotropic resolution with a mean percent difference in size of 26% (overall average  $1.62 \pm 0.70 \text{ g}$  versus  $1.18 \pm 0.52 \text{ g}$ ,  $p < 0.001$ , Cohen's  $d_z = 1.33$ ). The corresponding Bland-Altman plot showed a large bias for the difference in the peri-infarct gray zone size between using anisotropic resolution and isotropic resolution.

Figure 6 shows the relationships between LGE and isotropic MCLE measures of the infarct core and gray zone sizes of a short-axis slice with thickness on the order of 8 mm across 11 subjects. Agreement was observed in the measures of the infarct core size between conventional 2D LGE and isotropic 3D MCLE ( $r = 0.88, p = 0.12$ ), and no bias was detected using the Bland-Altman analysis. The peri-infarct gray zone size measured by conventional 2D LGE was significantly larger than that measured by isotropic 3D MCLE with a mean percent difference in size of 27% (overall average  $1.55 \pm 0.61 \text{ g}$  versus  $1.09 \pm 0.42 \text{ g}$ ,  $p = 0.0016$ , Cohen's  $d_z = 1.20$ ). The corresponding Bland-Altman plot demonstrated a large bias for the difference in the peri-infarct gray zone size between using conventional 2D LGE and isotropic 3D MCLE. Furthermore, over the same short-axis slice on each of 11 subjects, we respectively compared measures of the two infarct heterogeneity indices between conventional

	Total (n = 11)
Age (years)	$60 \pm 14$
Male (%)	5 (45.5)
Previous MI (%)	11 (100)
Heart rate (bpm)	$56 \pm 5$
Hypertension (%)	6 (54.5)
Diabetes (%)	1 (9)
Smoking (%)	1 (9)
Dyslipidemia (%)	6 (54.5)
LVEF (%)	$42 \pm 11$
LVEDV (ml)	$174 \pm 66$
LVESV (ml)	$103 \pm 56$

**TABLE 1** Baseline characteristics of the patient population

Abbreviations used in the table: LVEF (left ventricular ejection fraction); LVEDV (left ventricular end diastolic volume); LVESV (left ventricular end systolic volume); bpm (beats per minute)



**FIGURE 1** Imaging results for a representative short-axis slice of a patient with prior myocardial infarction. **A-F**, Multi-contrast images at varied TIs with an isotropic resolution of 2.2 mm. **g**: The corresponding LGE image with a resolution of  $1.37 \times 2.7 \times 8 \text{ mm}^3$

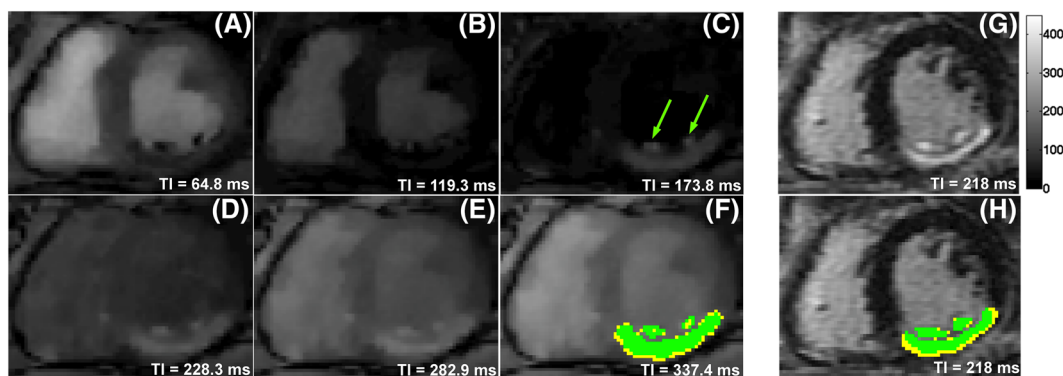


**FIGURE 2** Imaging and infarct segmentation results for a representative short-axis slice on a patient different from the one shown in Figure 1. **A-F**: MCLC images with an isotropic resolution of 2.2 mm. The green arrows in **c** point to the infarcted papillary muscle. The infarct segmentation result was overlaid to the magnitude image at the inversion time of 337.4 ms. **G**, The corresponding LGE image with a resolution of  $1.37 \times 2.7 \times 8 \text{ mm}^3$ . **H**, Infarct segmentation result for the corresponding LGE slice. Green and yellow indicated infarct core and gray zone, respectively

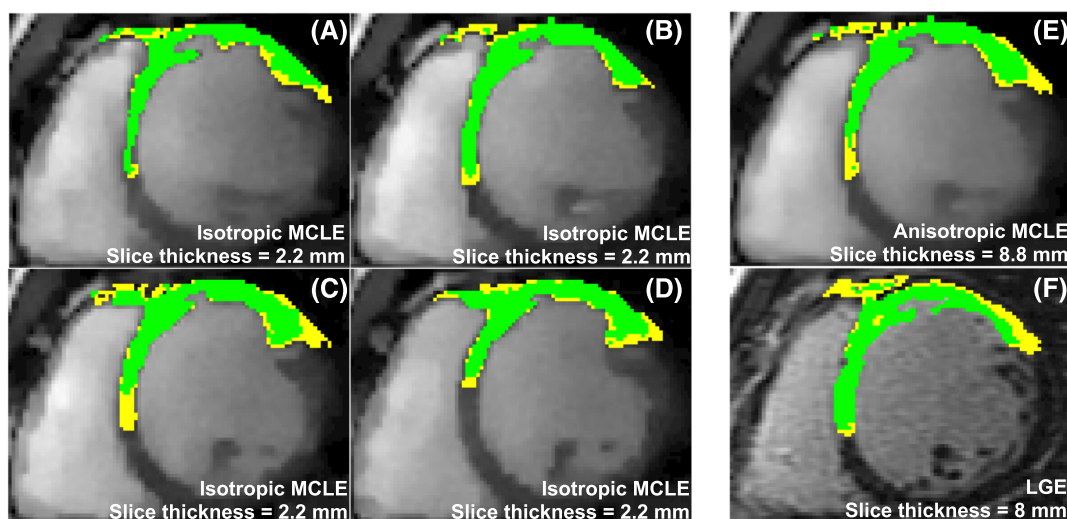


**FIGURE 3** Infarct core and peri-infarct gray zone segmentation results overlaid onto the magnitude images acquired using different methods for the same patient as in Figure 1. **A-D**, Infarct segmentation results for the central 4 consecutive slices of a short-axis slab using MCLC with an isotropic resolution of 2.2 mm (MCLC with  $\text{TI} = 60.8 \text{ ms}$  shown). **e**: Infarct segmentation result for the 8.8-mm-thick short-axis slice that corresponds to the 4 slices in **a-d** using MCLC with an anisotropic resolution of  $2.2 \times 2.2 \times 8.8 \text{ mm}^3$ . **F**, Infarct segmentation result for a corresponding LGE slice ( $\text{TI} = 240 \text{ ms}$ ) with a resolution of  $1.37 \times 2.7 \times 8 \text{ mm}^3$ . Green and yellow indicated infarct core and gray zone, respectively

2D LGE and anisotropic 3D MCLC (resolution =  $2.2 \times 2.2 \times 8.8 \text{ mm}^3$ ). There were no statistically significant differences between the measures of the infarct core ( $r = 0.89$ ,  $p = 0.07$ ) or peri-infarct gray zone ( $r = 0.78$ ,  $p = 0.19$ ) using conventional 2D LGE versus anisotropic 3D MCLC.

## 4 | DISCUSSION

In this work, we demonstrated the feasibility of applying accelerated 3D MCLC with isotropic resolution reconstructed using the CP-LASER technique to assess infarct heterogeneity in a clinical study of 11 post-infarction patients.

This study was performed at 1.5T; while 3T has better signal-to-noise ratio, in our feasibility studies performed on a 3T GE scanner using a swine model of chronic infarct<sup>28,29</sup> we observed more pronounced artifacts related to the IR balanced SSFP, as compared to the same sequence on 1.5T. In addition, ICDs are a consideration for this patient population and it will be difficult to scan them at 3T in the near future.

In the clinical study, we observed that for a given short-axis slab, the extent of the peri-infarct gray zone seemed to be overestimated by using anisotropic resolution compared to the measure derived from using higher isotropic resolution that is superior in the through-plane dimension. Pop et al also reported a similar observation from the quantitative analysis of the peri-infarct gray zone using 3D MCLC in an *ex vivo* preclinical study on a swine model of chronic infarction.<sup>16</sup> Arai et al demonstrated the measure of the peri-infarct gray zone size using 3D LGE in *ex vivo* rat hearts with chronic myocardial infarction varies inversely with spatial resolution.<sup>15</sup> Consistent with these exploratory preclinical research studies, our clinical findings further emphasize the potential utility of volumetric CMR with high spatial resolution in assessing infarct heterogeneity.

A previous clinical study of 15 post-infarct patients showed that: 1) using exactly the same anisotropic resolution, 2D MCLC using the fuzzy clustering method yielded similar measures for both infarct core size and peri-infarct gray zone size to 2D LGE using FWHM; 2) there was no

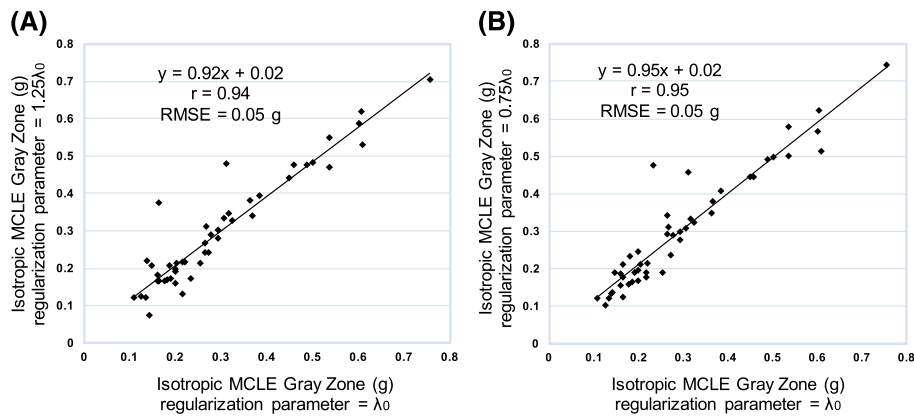


**FIGURE 4** MCLE measures in the gray zone size of an individual short-axis slice across 11 patient subjects with an isotropic resolution of 2.2 mm using different regularization parameters. **A**, Correlation in MCLE gray zone measures between using  $\lambda_0$  and a regularization parameter larger than  $\lambda_0$  by 25% ( $p = 0.81$ ). **B**, Correlation in MCLE gray zone measures between using  $\lambda_0$  and a regularization parameter smaller than  $\lambda_0$  by 25% ( $p = 0.31$ )

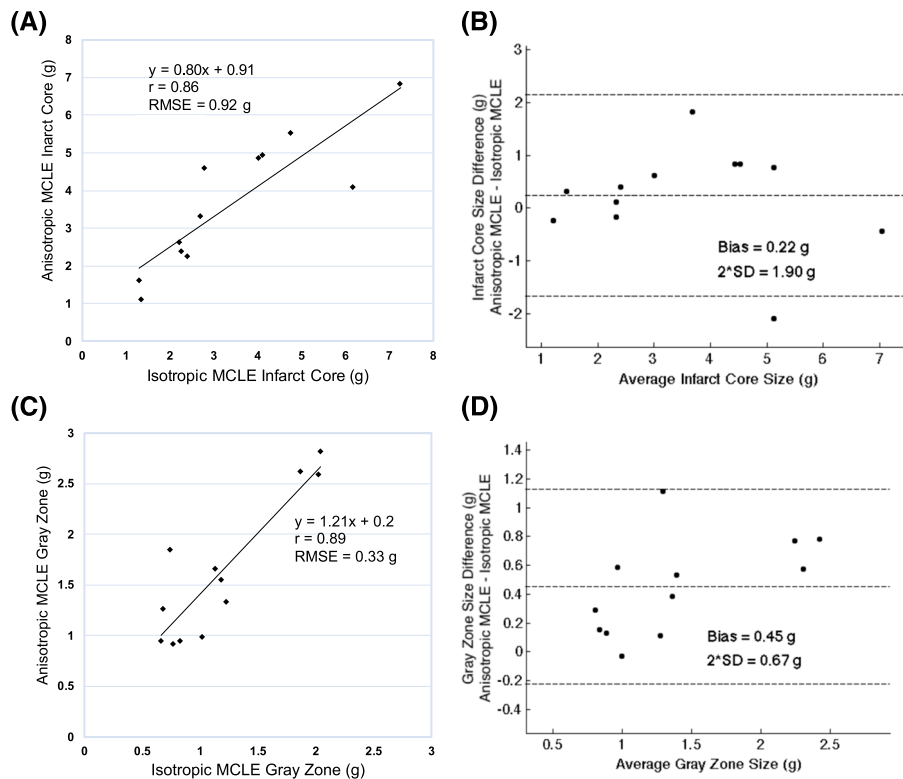


**FIGURE 5** Comparison of MCLE infarct core and gray zone measures for a 8.8-mm-thick short-axis slab using isotropic 2.2-mm resolution versus anisotropic resolution ( $2.2 \times 2.2 \times 8.8 \text{ mm}^3$ ) across 11 patient subjects. **A-B**, Regression analysis ( $p = 0.43$ ) and the corresponding Bland-Altman plot for MCLE infarct core measures. **C-D**, Regression analysis ( $p < 0.001$ ) and the corresponding Bland-Altman plot for MCLE gray zone measures

statistical difference when comparing the infarct core or peri-infarct gray zone sizes derived by the MCLE and LGE analysis.<sup>24</sup> In our study, we also made a comparison of infarct core and peri-infarct gray zone measures for corresponding short-axis slices using anisotropic 3D MCLE versus 2D LGE at similar spatial resolutions. Large effect sizes were only seen in the gray zone measurements between anisotropic MCLE and isotropic MCLE, and in the gray zone measurements between 2D LGE and isotropic MCLE. Our findings agree with the observations from the previous study: the infarct core and gray zone sizes measured by anisotropic 3D MCLE were statistically similar to the corresponding sizes measured by conventional 2D LGE. This means the differences in the gray zone size between high-resolution 3D MCLE and 2D LGE with thicker slices are primarily due to resolution rather than any differences in the ways gray zone is analyzed.

The use of manually drawn remote regions and manual epicardial and endocardial contours in the LGE analysis could add significant variability to the measure of the peri-infarct gray zone. Different remote zones in healthy myocardium, where noise dominates and the true signal intensity is approximately zero, can lead to variable lower-bound thresholds for defining the peri-infarct gray zone using FWHM. The determination of the peri-infarct gray zone pixels in the infarct-blood border area could also be greatly affected by differences in manually drawn endocardial contours, particularly when the signal intensity of the infarct is similar to that of adjacent blood. A previous study using low-resolution 2D MCLE ( $1.7 \times 1.7 \times 8 \text{ mm}^3$ ) reported that: 1) image noise has a bigger impact on peri-infarct gray zone variability using the LGE analysis (16%) than the MCLE analysis (4%); 2) a 12% variability in the measure of peri-infarct gray zone size was caused by differences in manual contouring across reviewers in the LGE analysis, and there were no manual contours used in the MCLE analysis.<sup>24</sup> In this study, mean percent difference in gray zone measurements was greater than 12% when comparing isotropic 3D MCLE to anisotropic 3D MCLE (26%), and isotropic 3D MCLE to 2D LGE (27%), showing a larger effect than the variability due to manual contouring.

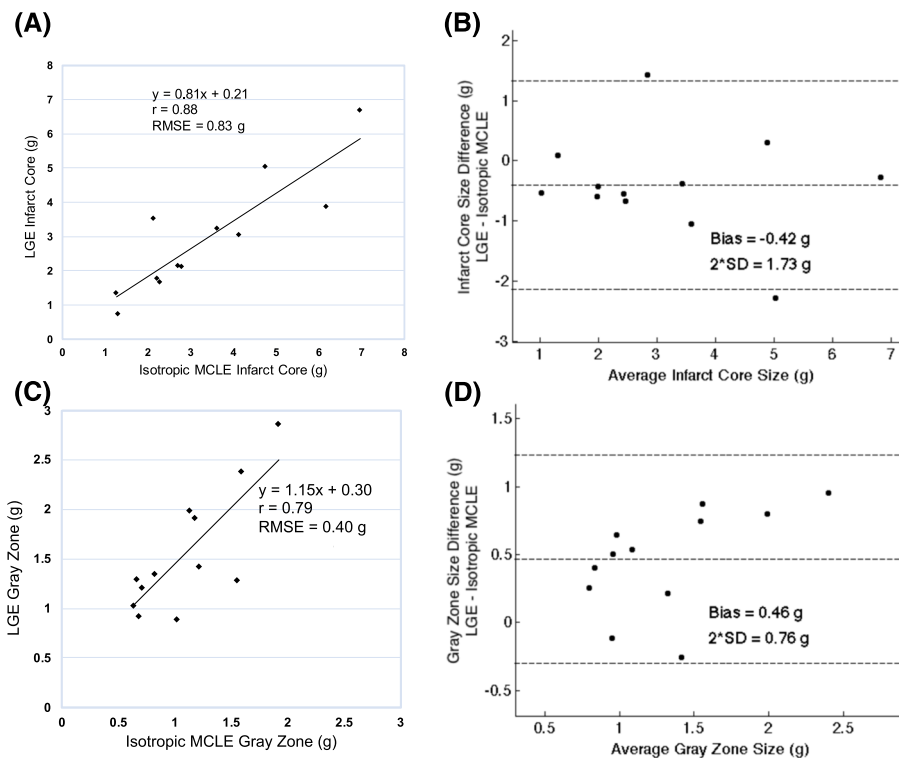


**FIGURE 6** Comparison of infarct core and gray zone measures for corresponding short-axis slices using MCLC with isotropic 2.2-mm resolution versus LGE (resolution =  $1.37 \times 2.7 \times 8 \text{ mm}^3$ ) across 11 patient subjects. **A–B:** Regression analysis ( $p = 0.12$ ) and the corresponding Bland-Altman plot for infarct core measures. **C–D:** Regression analysis ( $p = 0.0016$ ) and the corresponding Bland-Altman plot for gray zone measures

In this study, LGE was performed around 10 minutes after contrast bolus, and MCLC was performed 10–20 minutes after LGE. A previous study has shown that consistent measures in the infarct core or peri-infarct gray zone size were observed using two sets of LGE images acquired 10 minutes apart, and also indicated that reproducible quantification of infarct heterogeneity could be achieved between 20 and 30 minutes after contrast bolus.<sup>7</sup> Therefore, the effect of contrast kinetics on infarct heterogeneity assessment is likely to be negligible in this study. Furthermore, inconsistent breath-hold positions between LGE and MCLC scans could occur, adding variability to the following infarct heterogeneity assessment. However, when comparing anisotropic 3D MCLC and 2D LGE, the measures of the infarct core or peri-infarct gray zone demonstrated good agreement with no statistical difference. That being said, inconsistency in breath-hold positions between LGE and MCLC scans should primarily increase variability between MCLC and LGE scans, rather than introducing systemic bias.

Isotropic 3D MCLC has demonstrated advantages over conventional 2D LGE in assessing infarct heterogeneity. Firstly, isotropic 3D MCLC was able to capture variations in infarct characteristics across thin short-axis slices, which could not be identified using conventional 2D LGE. Secondly, with an isotropic resolution, assessment of infarct heterogeneity by 3D MCLC was less affected by partial volume effects than conventional 2D LGE. For a given infarct region, the peri-infarct gray zone size measured by isotropic 3D MCLC was significantly smaller than that measured by conventional 2D LGE, while the measures in the infarct core size by the two methods were similar. When the through-plane resolution of 3D MCLC was changed from 2.2 mm to 8.8 mm to be similar to that of conventional 2D LGE, the gray zone size measured by anisotropic 3D MCLC did not statistically differ from that measured by conventional 2D LGE. Since the peri-infarct region comprises a patchy mixture of viable myocytes and fibrotic bundles with different MR contrasts, where patch sizes are on the order of a few millimetres, the estimation of gray zone size attributable to this region is expected to be more sensitive to changes in imaging resolution when compared to regions of core infarct where the MR contrast is expected to be more uniform. As such, conventional 2D LGE using an inferior resolution would have likely overestimated the extent of the true heterogeneous mixture of infarct and healthy myocardium in this work. Lastly, the MCLC-derived infarct heterogeneity analysis is expected to be more reproducible than the LGE-derived counterpart, because the fuzzy clustering method requires no manual operator input and uses data fitting of signal intensities at different TIs, yielding parameters more directly reflective of contrast agent distribution, with reduced variability caused by image noise.<sup>24</sup>

Using CP-LASER accelerated 3D MCLC, volumetric infarct imaging in the short-axis view at an isotropic resolution of 2.2 mm with a long-axis coverage of 2.2 cm has been achieved in a single breath-hold scan. A recent clinical study demonstrated the feasibility of using low-dimensional-structure self-learning and thresholding (LOST) accelerated 3D LGE to assess myocardial viability, where a long-axis coverage of 10 cm with a high isotropic resolution of 1.4–1.7 mm was implemented in a navigator-gated free-breathing scan of 4–6 minutes with a fixed navigator efficiency of 60%.<sup>34,35</sup> Similarly, the CP-LASER accelerated 3D MCLC would be able to achieve a clinically favourable isotropic resolution of 1.5 mm while increasing long-axis coverage to 10 cm using short navigator-gated free-breathing scans of 4–5 minutes assuming a navigator efficiency of 50–60%.

To evaluate the performance of isotropic 3D MCLC in infarct heterogeneity assessment, we compared to conventional 2D LGE rather than 3D LGE, as 2D LGE has been considered as the clinical gold standard for infarction visualization, and is widely used to quantify infarct heterogeneity



in a variety of clinical settings.<sup>7-9</sup> On the other hand, fully-sampled 3D LGE usually requires a very long acquisition time resulting in a contrast washout issue, and 3D LGE using acceleration techniques at a high acceleration rate  $> 4$  is not yet widely available or extensively tested for clinical utility in peri-infarct imaging.

Although isotropic 3D MCLE has demonstrated the potential to more accurately assess infarct heterogeneity, our findings on post-infarction patients lack direct correspondence with clinical outcomes. In a recent retrospective clinical study of 27 post-infarction patients with preventative ICD implantation, inferior spatial resolution caused an increased CMR measure in the peri-infarct gray zone, leading to reduced sensitivity in predicting appropriate ICD therapy.<sup>36</sup> As indicated by this research, with a high isotropic resolution, 3D MCLE should be able to provide more precise assessment of infarct heterogeneity, which would potentially be better correlated with appropriate ICD therapy.

In the absence of commercially available 3D MCLE, high resolution 3D LGE methods should be used in clinical routine for scar-imaging in post-MI patients where these methods are readily implemented as in.<sup>17,18</sup> Also, although we did not perform a head-to-head comparison between 3D MCLE and 3D LGE, we suggest that based on current results, 3D MCLE can perform more robustly with respect to infarct delineation due to: 1) the multi-contrast nature of the technique which allows us to extract  $T_1$  steady-state maps instead of trial- and error-based optimization of inversion times for LGE acquisition, as well as to obtain a superior CNR between tissue types (infarct-blood, infarct-healthy myocardium) and better detection of subendocardial VT substrate as compared to LGE methods; and 2) the elimination of uncertainties and unreproducible results associated with SI thresholds and tedious epicardial/endocardial manual contouring as in LGE analysis.

The utility of isotropic 3D MCLE to improve clinical outcome on post-infarction patients needs to be further evaluated in more extensive clinical studies with either short-term or long-term follow-up. Given the encouraging preliminary results in this pilot patient study, we propose next a study using 3D MCLE and 3D LGE with a high isotropic resolution covering the infarct territory to compute the total size of the peri-infarct gray zone in post-infarction patients prior to ICD implantation as a complementary index, facilitating risk stratification based on correlation with appropriate ICD firing, particularly for those patients with preserved LVEF. The 3D distribution of infarct core and peri-infarct gray zone could also be applied to model and simulate the re-entrant substrate, thereby predicting the inducibility of ventricular arrhythmias.

## 5 | CONCLUSION

In conclusion, clinical infarct heterogeneity assessment would benefit from multi-contrast volumetric imaging with isotropic resolution, which enables detecting smaller peri-infarct structures and facilitates more accurate peri-infarct gray zone measurement. Isotropic 3D MCLE provides better delineation of infarct morphology and improved infarct heterogeneity assessment on post-infarction patients compared to conventional 2D LGE.

## ACKNOWLEDGMENTS

The authors thank Rhonda Walcarius and Mary Li for help with patient studies, and Labonny Biswas for assistance with manuscript revisions.

## FUNDING

Funding provided by GE Healthcare, the Ontario Research Fund and the Canadian Institutes of Health Research grant MOP-93531.

## COMPETING INTERESTS

Dr. Wright receives research support from GE Healthcare. The authors declare no other competing interests.

## AUTHORS' CONTRIBUTIONS

- LZ: study design, image reconstruction and analysis, drafted manuscript.
- LP: critically reviewed the manuscript. IR: patient demographic data collection, measured LV functional parameters.
- MP: critically reviewed the manuscript.
- GAW: guided study design, data analysis and interpretation; critically reviewed the manuscript.

## ETHICS APPROVAL AND CONSENT TO PARTICIPATE

Studies were approved by the Research Ethics Board at Sunnybrook Health Sciences Centre. Informed consent was obtained in all subjects.

## AVAILABILITY OF DATA AND MATERIAL

The datasets used in this study are available from the corresponding author on reasonable request.

## ORCID

Li Zhang  <https://orcid.org/0000-0003-0794-0276>

## REFERENCES

1. Fishman GI, Chugh SS, DiMarco JP, et al. Sudden cardiac death prediction and prevention: report from a national heart, lung, and blood institute and heart rhythm society workshop. *Circ*. 2010;122(22):2335–2348.
2. John RM, Tedrow UB, Koplman BA, et al. Ventricular arrhythmias and sudden cardiac death. *Lancet*. 2012;380(9852):1520–1529.
3. Myerburg RJ. Implantable cardioverter–defibrillators after myocardial infarction. *New England J Med*. 2008;359(21):2245–2253.
4. Russo AM, Stainback RF, Bailey SR, et al. Accf/hrs/aha/ase/hfsa/scai/scct/scmr 2013 appropriate use criteria for implantable cardioverter–defibrillators and cardiac resynchronization therapy: A report of the american college of cardiology foundation appropriate use criteria task force, heart rhythm society, american heart association, american society of echocardiography, heart failure society of america, society for cardiovascular angiography and interventions, society of cardiovascular computed tomography, and society for cardiovascular magnetic resonance. *Heart Rhythm*. 2013;10(4):e11–e58.
5. Bardy GH, Lee KL, Mark DB, et al. Amiodarone or an implantable cardioverter–defibrillator for congestive heart failure. *New England J Med*. 2005;352(3):225–237.
6. Sabir IN, Usher-Smith JA, Huang CL-H, Grace AA. Risk stratification for sudden cardiac death. *Progress Biophysics Molecular Biol*. 2008;98(2–3):340–346.
7. Schmidt A, Azevedo CF, Cheng A, et al. Infarct tissue heterogeneity by magnetic resonance imaging identifies enhanced cardiac arrhythmia susceptibility in patients with left ventricular dysfunction. *Circ*. 2007;115(15):2006–2014.
8. Roes SD, Borleffs CJW, van der Geest RJ, et al. Infarct tissue heterogeneity assessed with contrast-enhanced magnetic resonance imaging predicts spontaneous ventricular arrhythmia in patients with ischemic cardiomyopathy and implantable cardioverter–defibrillator. *Circ : Cardiovascular Imaging*. 2009; 2(3):183–190.
9. Rayatzadeh H, Tan A, Chan RH, et al. Scar heterogeneity on cardiovascular magnetic resonance as a predictor of appropriate implantable cardioverter defibrillator therapy. *J Cardiovascular Mag Res*. 2013;15(1):31.
10. Lee DC, Goldberger JJ. Cmr for sudden cardiac death risk stratification. *JACC: Cardiovascular Imag*. 2013;3(6):345–348.
11. Zeidan-Shwiri T, Yang Y, Lashevsky I, et al. Magnetic resonance estimates of the extent and heterogeneity of scar tissue in icd patients with ischemic cardiomyopathy predict ventricular arrhythmia. *Heart Rhythm*. 2015;12(4):802–808.
12. Disertori M, Rigoni M, Pace N, et al. Myocardial fibrosis assessment by lge is a powerful predictor of ventricular tachyarrhythmias in ischemic and nonischemic lv dysfunction: a meta-analysis. *JACC: Cardiovascular Imag*. 2016;9(9):1046–1055.
13. Perez-David E, Arenal Á, Rubio-Guivernau JL, et al. Noninvasive identification of ventricular tachycardia-related conducting channels using contrast-enhanced magnetic resonance imaging in patients with chronic myocardial infarction: comparison of signal intensity scar mapping and endocardial voltage mapping. *J Amer College Cardiology*. 2011;57(2):184–194.
14. Ashikaga H, Sasano T, Dong J, et al. Magnetic resonance–based anatomical analysis of scar-related ventricular tachycardia: implications for catheter ablation. *Circ Res*. 2007;101(9):939–947.
15. Schelbert EB, Hsu L-Y, Anderson SA, et al. Late gadolinium-enhancement cardiac magnetic resonance identifies postinfarction myocardial fibrosis and the border zone at the near cellular level in ex vivo rat heart/clinical perspective. *Circ: Cardiovascular Imag*. 2010;3(6):743–752.
16. Pop M, Ramanan V, Yang F, Zhang L, Newbigging S, Ghugre N, Wright G. High-resolution 3-d t1\*–mapping and quantitative image analysis of gray zone in chronic fibrosis. *IEEE Trans Biomed Eng*. 2014;61(12):2930–2938.
17. Fernández-Armenta J, Berruzo A, Andreu D, et al. Three-dimensional architecture of scar and conducting channels based on high resolution ce-cmr: insights for ventricular tachycardia ablation. *Circ Arrhythm Electrophysiol*. 2013;6(3):528–537.
18. Andreu D, Ortiz-Perez JT, Fernandez-Armenta J, et al. 3d delayed-enhanced magnetic resonance sequences improve conducting channel delineation prior to ventricular tachycardia ablation. *EP Europace*. 2015;17(6):938–945.
19. Kim RJ, Fieno DS, Parrish TB, et al. Relationship of mri delayed contrast enhancement to irreversible injury, infarct age, and contractile function. *Circ*. 1999;100(19):1992–2002.
20. Kim RJ, Wu E, Rafael A, et al. The use of contrast-enhanced magnetic resonance imaging to identify reversible myocardial dysfunction. *New England J Med*. 2000;343(20):1445–1453.
21. Yan AT, Shayne AJ, Brown KA, et al. Characterization of the peri-infarct zone by contrast-enhanced cardiac magnetic resonance imaging is a powerful predictor of post–myocardial infarction mortality. *Circ*. 2006;114(1):32–39.
22. Heidary S, Patel H, Chung J, et al. Quantitative tissue characterization of infarct core and border zone in patients with ischemic cardiomyopathy by magnetic resonance is associated with future cardiovascular events. *J Amer College Cardiology*. 2010;55(24):2762–2768.
23. Detsky J, Stainsby J, Vijayaraghavan R, Graham J, Dick A, Wright G. Inversion-recovery-prepared ssfp for cardiac-phase-resolved delayed-enhancement mri. *Magn Res Med*. 2007;58(2):365–372.
24. Detsky J, Paul G, Dick AJ, Wright GA. Reproducible classification of infarct heterogeneity using fuzzy clustering on multicontrast delayed enhancement magnetic resonance images. *IEEE Trans Med Imaging*. 2009;28(10):1606–1614.
25. Connelly K, Detsky J, Graham JJ, Paul G, Vijayaragavan R, Dick AJ, Wright GA. Multicontrast late gadolinium enhancement imaging enables viability and wall motion assessment in a single acquisition with reduced scan times. *J Magn Res Imaging*. 2009;30(4):771–777.
26. Yang Y, Connelly K, Graham JJ, Detsky J, Lee T, Walcarius R, Paul G, Wright GA, Dick AJ. Papillary muscle involvement in myocardial infarction: Initial results using multicontrast late-enhancement mri. *J Magn Res Imag*. 2011;33(1):211–216.
27. Yang Y, Connelly K, Zeidan-Shwiri T, et al. Multi-contrast late enhancement cmr determined gray zone and papillary muscle involvement predict appropriate icd therapy in patients with ischemic heart disease. *J Cardiovascular Magn Res*. 2013;15(1):57.
28. Zhang L, Athavale P, Pop M, Wright GA. Multicontrast reconstruction using compressed sensing with low rank and spatially varying edge-preserving constraints for high-resolution mr characterization of myocardial infarction. *Magn Res Med*. 2016;78(2):598–610.
29. Zhang L, Lai P, Pop M, Wright GA. Accelerated multicontrast volumetric imaging with isotropic resolution for improved peri-infarct characterization using parallel imaging, low-rank and spatially varying edge-preserving sparse modeling (2017). *Magnetic Reson Med*. 2018;79(6):3018–3031.

30. Uecker M, Lai P, Murphy MJ, Virtue P, Elad M, Pauly JM, Vasanawala SS, Lustig M. Espirit – an eigenvalue approach to autocalibrating parallel mri: Where sense meets grappa. *Magnetic Reson Med*. 2014;71(3):990–1001.
31. Roifman I, Ghugre NR, Vira T, et al. Assessment of the longitudinal changes in infarct heterogeneity post myocardial infarction. *BMC Cardiovasc Disord*. 2016;16(198).
32. Pop M, Ghugre NR, Ramanan V, Morikawa L, Stanisz G, Dick AJ, Wright GA. Quantification of fibrosis in infarcted swine hearts by ex vivo late gadolinium-enhancement and diffusion-weighted mri methods. *Phys Med Biology*. 2013;58(15):5009–5028.
33. Ghugre NR, Ramanan V, Pop M, Yang Y, Barry J, Qiang B, Connelly K, Dick AJ, Wright GA. Quantitative tracking of edema, hemorrhage, and microvascular obstruction in subacute myocardial infarction in a porcine model by mri. *Magn Res Med*. 2011;66(4):1129–1141.
34. Akçakaya M, Rayatzadeh H, Basha TA, et al. Accelerated late gadolinium enhancement cardiac mr imaging with isotropic spatial resolution using compressed sensing: initial experience. *Radiology*. 2012;264(3):691–699.
35. Basha TA, Akçakaya M, Liew C, et al. Clinical performance of high-resolution late gadolinium enhancement imaging with compressed sensing. *J Magn Reson Imaging*. 2017;46(6):1829–1838.
36. Farrag NA, Ramanan V, Wright GA, Ukwatta E. Effect of t1-mapping technique and diminished image resolution on quantification of infarct mass and its ability in predicting appropriate icd therapy. *Med Physics*. 2018;45(4):1577–1585.

**How to cite this article:** Zhang L, Lai P, Roifman I, Pop M, Wright GA. Multi-contrast volumetric imaging with isotropic resolution for assessing infarct heterogeneity: Initial clinical experience. *NMR in Biomedicine*. 2020;33:e4253. <https://doi.org/10.1002/nbm.4253>